CMUT Ring Arrays for Forward-Looking Intravascular Imaging

Ömer Oralkan, Sean T. Hansen, Barış Bayram, Göksen G. Yaralıoğlu, A. Sanlı Ergun, and Butrus T. Khuri-Yakub

E. L. Ginzton Laboratory
Stanford University
Stanford, CA 94305-4088, U.S.A.

***Abstract*— This paper describes an annular CMUT ring array designed and fabricated for the tip of a catheter used for forward-looking intravascular imaging. A 64-element, 2-mm average diameter array is fabricated as an experimental prototype. A single element in the array is connected to a single-channel custom front-end integrated circuit for pulse-echo operation. In conventional operation the transducer operated at around 10 MHz. In the collapsed regime, the operating frequency shifted to 25 MHz and the received echo amplitude tripled. The SNR is measured as 23 dB in a 50-MHz measurement bandwidth for an echo signal from a plane reflector at 1.5 mm. We also performed a nonlinear dynamic transient finite element analysis for the described transducer, and found these results are in good agreement with the experimental measurements, both for conventional and collapsed operation.**

I. INTRODUCTION

Intravascular ultrasound (IVUS) has become a valuable diagnostic tool for many intravascular interventions (e.g., aortic aneurysm repair, stent placement, management of iliac vein compression) [1]. IVUS imaging probes have evolved from mechanically rotated single transducers to arrays enabling the electronic scanning of the cross-sectional area around a catheter [2]. However, current 1-D side-looking (SL) ultrasound imaging arrays do not have forward viewing capability to guide interventions. In addition, since blood flow is perpendicular to the image plane of SL arrays, Doppler-based flow measurement cannot be used in these systems. Forward-looking (FL) imaging is a complementary IVUS modality that has potential for guiding therapeutic and diagnostic interventions.

Ideally, a fully populated disk transducer array would provide the best solution for forward-looking capability. However, the use of a disk transducer array is not compatible with the guide wire used in catheter delivery systems. The guiding wire extends beyond the catheter tip, preventing the use of a full aperture array. Alternatively, an annular array (with same outer and inner diameters as the catheter itself) can be placed at the catheter tip, creating a forward-looking capability without obstructing the guiding wire.

Significant research efforts have been devoted to the development of forward-looking ring arrays [3]. However, these efforts are yet to result in a practical, clinically useful system, mainly due to difficulties stemming from the existing transducer and interconnect technologies. Capacitive micromachined ultrasonic transducer (CMUT) arrays are fabricated using standard integrated circuit (IC) fabrication techniques; complex geometries can, therefore, be implemented by simple lithographic steps. Hundreds of arrays can be fabricated at one time on a single silicon wafer. These transducers are inherently wideband, and provide sensitivity comparable to piezoelectric transducers [4, 5]. Another important attribute of CMUT technology (especially critical for intravascular applications) is its potential for integrating transducer arrays and supporting electronic circuits in a

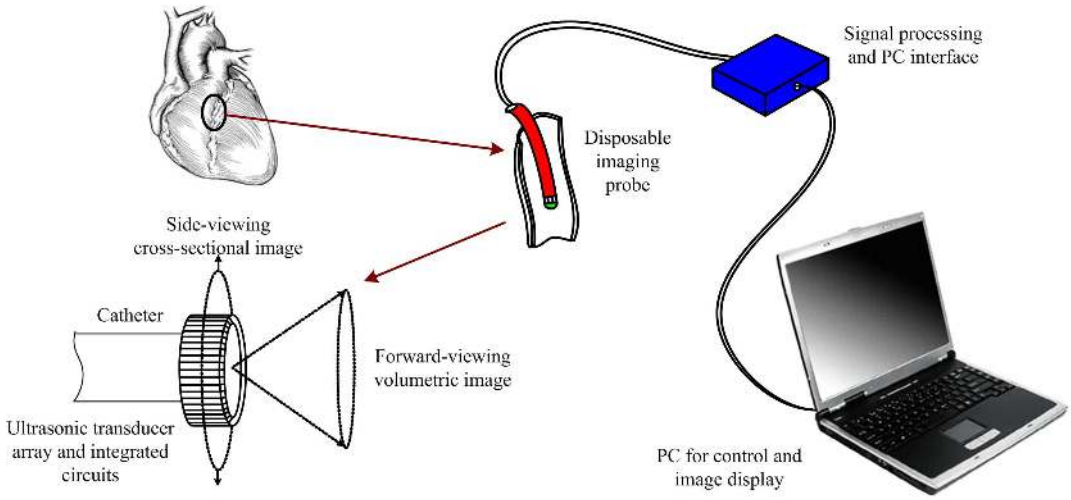

Fig. 1. A conceptual drawing of an integrated intravascular ultrasound imaging system.

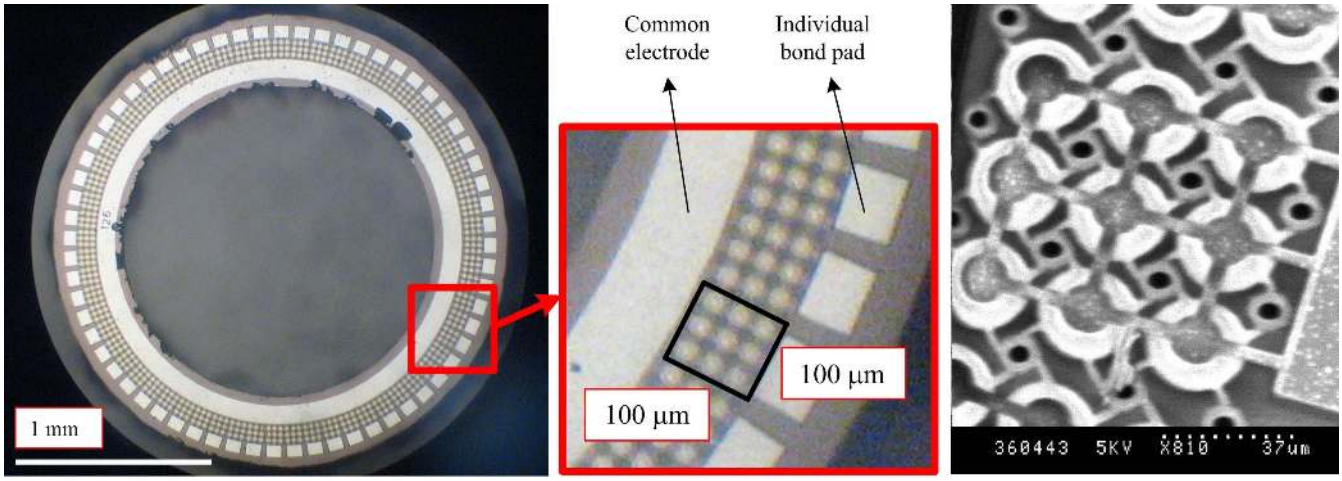

Fig. 2. (a) Top view of the 64-element CMUT ring array. (b) Magnified view of individual element (c) SEM photograph of a single element comprising 9 circular membranes.

TABLE I. PHYSICAL PARAMETERS OF THE CMUT RING ARRAY

Outer diameter, *mm*	2.4
Inner diameter, *mm*	1.6
Size of an element, *µm*	100 x 100
Element pitch (*d*), *µm*	100
Number of cells per element	9
Cell radius (r_{cell}), *µm*	13
Electrode radius (r_{el}), *µm*	6.5
Cell center spacing (d_{cell}), *µm*	31
Metal electrode thickness (t_e), *µm*	0.3
Membrane thickness (t_m), *µm*	0.4
Gap thickness (t_g), *µm*	0.15
Insulating layer thickness (t_i), *µm*	0.08
Silicon substrate thickness, *µm*	500
Number of elements per array	64

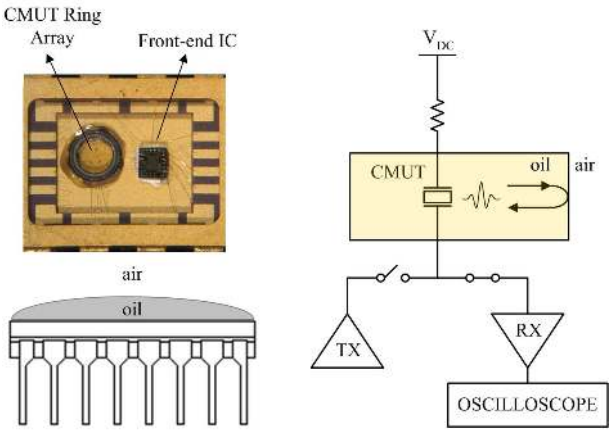

Fig. 3. Experimental pulse-echo setup.

compact form [6]. Our vision for an integrated intravascular imaging system is summarized in Fig. 1, where SL and FL CMUT arrays are integrated with the front-end electronic circuits in the probe at the tip of a catheter. This probe is connected to an external programmable signal processing unit that is interfaced to a general purpose personal computer.

In this paper, we present a 64-element CMUT annular ring array and preliminary pulse-echo results, obtained using a single channel custom integrated front-end ultrasonic transceiver wire-bonded to a single 100-µm x 100-µm element of the array.

II. CMUT ANNULAR RING ARRAYS

We have previously reported on CMUT ring arrays where a tented membrane structure was employed [7, 8]. Other researchers have also reported on the fabrication of similar arrays [9]. These arrays were not finalized in the form of a completely diced ring, and off-the-shelf electronic components were used to test them. As a result, the performance of CMUT ring arrays with very small elements could not be accurately assessed.

CMUT ring arrays presented in this paper are fabricated using the conventional surface micromachining process. The membrane and insulation layer materials are silicon nitride. Following the conventional fabrication process for CMUTs, deep through-wafer trenches are etched all around the array, using deep reactive ion etching. This process is also employed during the fabrication of 2-D CMUT arrays to form the through-wafer via interconnects [6]. At the end of this process step, the ring arrays are formed. The rings are connected to the wafer with thin support structures that would be easily broken prior to packaging.

The images of the resulting CMUT array are shown in Fig. 2. The physical dimensions of this array and its individual elements are summarized in Table I.

III. EXPERIMENTAL WORK

We placed the 64-element CMUT ring array into the cavity of a standard DIP-16 package, along with the front-end IC that comprises a pulse driver, a T/R switch, a wideband low-noise preamplifier, and an output buffer to drive off-chip loads. This

circuit was fabricated in a standard 0.25-µm standard CMOS process with a 2.5-V nominal supply voltage, and occupies an active silicon area of 70-µm x 70-µm. The electrical connections between a single 100-µm x 100-µm element, the front-end IC, and the package pins were provided by wire bonding. A photograph of the package is shown in Fig. 3(a). The CMUT ring array was immersed in vegetable oil, so that an oil-air interface was formed 1.5 mm away from the transducer, as shown in Fig. 3(b). The transducer was biased using a high-voltage DC power supply (model PS310 Stanford Research Systems, Inc., Sunnyvale, CA); a 5-V unipolar pulse with variable width was used for excitation. The received echo signals were sampled at a rate of 1 GSa/s, and digitized with an 8-bit resolution by a digitizing oscilloscope (model 54825A,

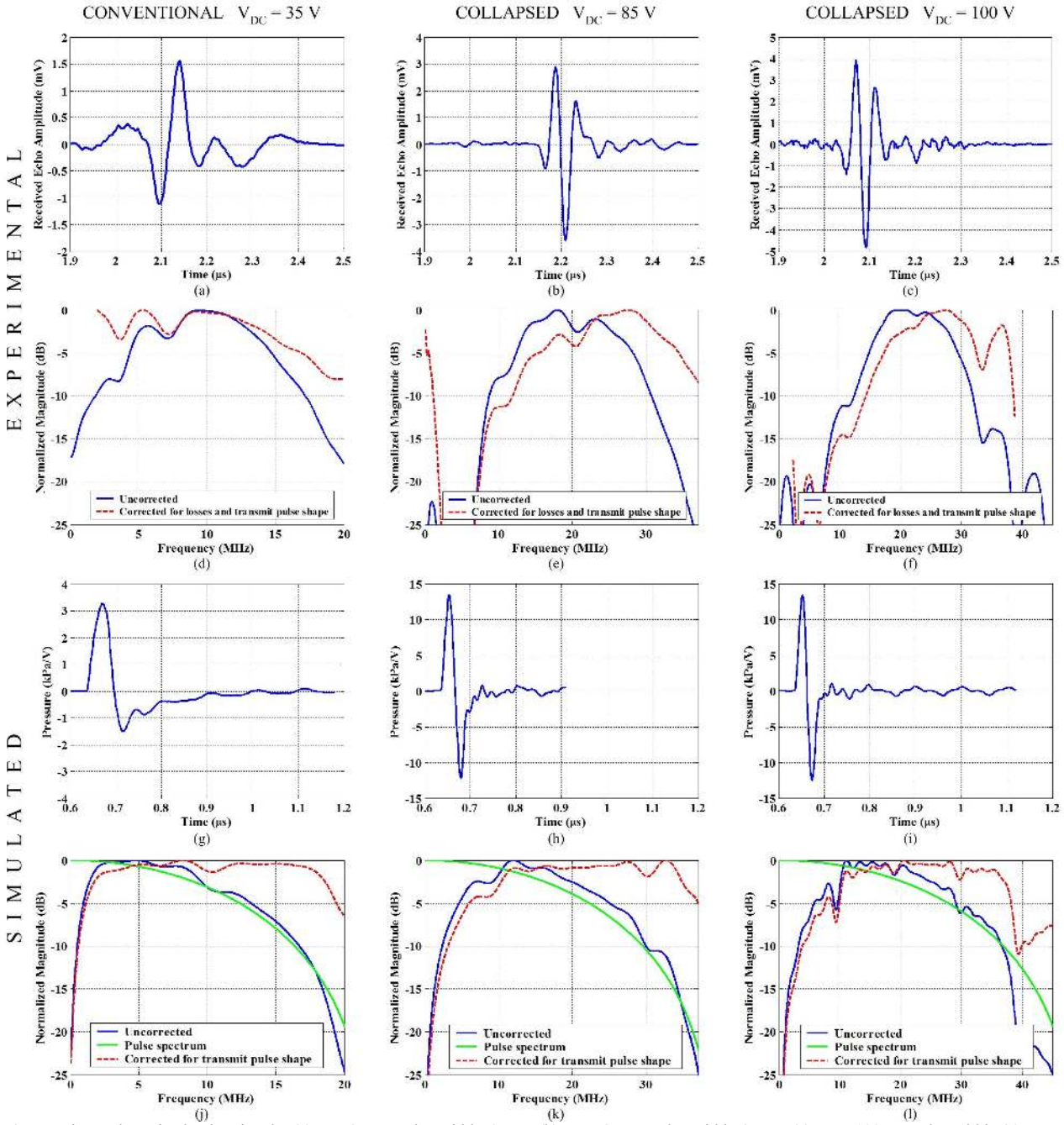

Fig 4. Experimental received echo signals: (a)V_{DC}=35 V, pulse width=45 ns, (b) V_{DC}=85 V, pulse width=25 ns, (c) V_{DC}=100 V, pulse width=20 ns; Fourier transform of the received echo signal, both before and after being corrected for diffraction and attenuation losses and the transmit pulse shape: (d) V_{DC}=35 V, pulse width=45 ns, (e) V_{DC}=85 V, pulse width=25 ns, (f) V_{DC}=100 V, pulse width=20 ns; Transmit pressure output waveforms obtained from nonlinear dynamic finite element analysis (g) V_{DC}=35 V, pulse width = 45 ns, (h) V_{DC}=85 V, pulse width=25 ns, (i) V_{DC}=100 V, pulse width=20 ns; Corresponding Fourier transforms both before and after being corrected for transmit pulse shape (j) V_{DC}=35 V, pulse width=45 ns, (k) V_{DC}=85 V, pulse width=25 ns, (l) V_{DC}=100 V, pulse width=20 ns;

TABLE II. COMPARISON OF EXPERIMENTAL AND SIMULATED RESULTS

			Experimental (Pulse-echo)			Nonlinear Dynamic Finite Element Analysis (Transmit only)		
V_{DC} (V)	Excitation	Operation Regime	f_0 (MHz)	6-dB BW (MHz)	Echo Amplitude (mV_{pp})	f_0 (MHz)	3-dB BW (MHz)	Pressure Output (kPa_{pp}/V)
35	-5 V, 45 ns	Conventional	9.8	15.9	2.6	10.2	17.2	4.7
85	-5 V, 25 ns	Collapsed	24.4	21.2	6.5	22.6	25.1	25.6
100	-5 V, 20 ns	Collapsed	27.3	21.5	8.8	23.9	27.0	25.8

Hewlett-Packard Co., Palo Alto, CA). A schematic representation of the experimental setup is shown in Fig. 3(c).

First, the array element is biased at 35 V (below its collapse voltage) and operated in the conventional regime. Then we increased the bias voltage above the collapse voltage, first to 85 V, and then further to 100 V. The received echo signals and corresponding Fourier transforms are shown in Fig. 4(a),(b),(c) and (d),(e),(f), respectively. These figures show that the pulse-echo echo amplitude is three times larger in collapsed operation than in conventional operation. The operating frequency also shifts from around 10 MHz to close to 25 MHz. A static finite element analysis has previously shown that collapsed operation of CMUTs results in a higher coupling efficiency and higher acoustic pressures, compared to conventional regime [10]. In this study, we conducted a nonlinear transient dynamic finite element analysis to accurately simulate the response of the CMUT ring array element to a unipolar excitation pulse. We set the DC bias voltage, and the pulse width and amplitude to be the same as the experiments. Because of the availability of enhanced contact capabilities and explicit time domain solver we chose to use LS-DYNA (Livermore Software Technology Corporation, Livermore, CA) in the finite element calculations [11]. The transient output pressure waveforms and corresponding Fourier transforms are shown in Fig. 4(g),(h),(i) and (j),(k),(l), respectively, for different bias conditions and excitations. The measurements on the experimental and simulated results are summarized in Table II. The 6-dB bandwidth is listed for the pulse-echo experimental results; the 3-dB bandwidth is used for transmit-only finite element analysis. The experimental frequency characteristics are in good agreement with the simulated results. The measured pulse-echo amplitude and the simulated peak output pressure also show the same increasing trend with increasing bias voltages.

We measured the SNR for the signal shown in Fig. 4(c) as 23 dB with no signal averaging in a 50-MHz measurement bandwidth. Given the 5-V excitation pulse amplitude, this signal quality is excellent, especially for an application where the required penetration depth is less than a centimeter.

IV. CONCLUSION

The preliminary results presented in this paper show that CMUT technology provides a means to fabricate arrays with different geometries and small size. These arrays, combined with custom integrated front-end circuits, demonstrate excellent signal quality at high frequencies. The collapsed operation that has been experimentally demonstrated here offers additional design and operating flexibility and improved performance. CMUT technology will enable the implementation of integrated intravascular imaging systems with improved image quality and additional functionality, empowering new procedures in interventional cardiology.

ACKNOWLEDGMENT

This work was supported by the National Institutes of Health. The authors would like to thank National Semiconductor Corporation for the fabrication of the prototype front-end integrated circuits.

REFERENCES

[1] P. G. Yock and P. J. Fitzgerald,, "Intravascular ultrasound: State of the art and future directions," *Am. J. Cardiol.*, vol. 81, pp. 27E-32E, Apr. 9, 1998.

[2] M. O'Donnell et al., "Catheter arrays: Can intravascular ultrasound make a difference in imaging coronary artery disease," in *Proc. IEEE Ultrason. Symp.*, 1997, pp. 1447-1456.

[3] Y. Wang, D. N. Stephens, and M. O'Donnell, "Optimizing the beam pattern of a forward-viewing ring-annular ultrasound array for intravascular imaging," *IEEE Trans. Ultrason., Ferroelect., Freq. Cont.*, vol. 49, pp. 1652-1664, Dec. 2002.

[4] Ö. Oralkan, X. C. Jin, F. L. Degertekin, and B. T. Khuri-Yakub, "Simulation and Experimental Characterization of a 2-D Capacitive Micromachined Ultrasonic Transducer Array Element," *IEEE Trans. Ultrason., Ferroelect., Freq. Cont.*, vol. 46, pp. 1337-1340, Nov. 1999.

[5] Ö. Oralkan et al., "Capacitive micromachined ultrasonic transducers: Next-generation arrays for acoustic imaging?," *IEEE Trans. Ultrason., Ferroelect., Freq. Cont.*, vol. 49, no. 11, pp. 1596-1610, Nov. 2002.

[6] Ö. Oralkan et al., "Volumetric Ultrasound Imaging Using 2-D CMUT Arrays," *IEEE Trans. Ultrason., Ferroelect., Freq. Cont.*, vol. 50, no. 11, pp. 1581-1594, Nov. 2003.

[7] A. S. Ergun et al., "Broadband capacitive micromachined ultrasonic transducers ranging from 10 kHz to 60 MHz for imaging arrays and more," in *Proc. IEEE Ultrason. Symp.*, 2002, pp. 1039–1043.

[8] U. Demirci, A. S. Ergun, Ö. Oralkan, M. Karaman, B. T. Khuri-Yakub, "Forward-viewing CMUT arrays for medical imaging," *IEEE Trans. Ultrason., Ferroelect., Freq. Cont.*, vol. 51, no. 7, pp. 887-895, Jul. 2004.

[9] J. G. Knight and F. L. Degertekin, "Fabrication and characterization of cMUTs for forward looking intravascular ultrasound imaging," in *Proc. IEEE Ultrason. Symp.*, 2002, pp. 577-580.

[10] B. Bayram, E. Hæggström, G. G. Yaralioglu, and B. T. Khuri-Yakub, "A New Regime for Operating Capacitive Micromachined Ultrasonic Transducers, *IEEE Trans. Ultrason., Ferroelect., Freq. Cont.*, vol. 50, no. 9, pp. 1184-1190, Sep. 2003.

[11] B. Bayram, G. G. Yaralioglu, A. S. Ergun, Ö. Oralkan, and B. T. Khuri-Yakub, "Dynamic FEM analysis of multiple CMUT cells in immersion," presented at the IEEE Intl. Ultrason. Symp., Montreal, Canada, 2004.